Catalysis Science & Technology

Accepted Manuscript

ROYAL SOCIETY OF CHEMISTRY

www.rsc.org/catalysis

ARTICLE TYPE www.rsc.org/xxxxxx | XXXXXXXX

Enantioselective 1,2-reductions of β-trifluoromethylated-α,β-unsaturated ketones to chiral allylic alcohols over organoruthenium-functionalized mesoporous silica nanospheres

Meng Wu, Lingyu Kong, Kaiwen Wang, Ronghua Jin, Tanyu Cheng, Guohua Liu*

Received (in XXX, XXX) Xth XXXXXXXXX 200X, Accepted Xth XXXXXXXXX 200X
First published on the web Xth XXXXXXXXX 200X
DOI: 10.1039/b000000x

Organoruthenium-functionalized mesoporous silica nanospheres are prepared through the co-assembly of chiral 4-(trimethoxysilyl)ethyl)phenylsulfonyl-1,2-diphenylethylene-diamine and tetraethoxysilane followed by complexation with an organoruthenium complex. Structural analysis and characterization disclose its well-defined single-site organoruthenium active center, and electron microscopy images reveal its uniformly distributive, mesostructured nanospheres. As a heterogenous catalyst, it displays high catalytic activity and enantioselectivity in the asymmetric 1,2-reductions of β-trifluoromethylated-α,β-unsaturated ketones to give chiral allylic alcohols, resulting in up to 97% enantioselectivity with a wide scope of substrates. Furthermore, this heterogeneous catalyst can be conveniently recovered and reused for at least eight times without loss of catalytic activity, showing particularly attractive in the practice of organic synthesis.

1. Introduction

Immobilization as a classical strategy is used extensively to solve the problem of transition-metal catalyst recycling, whilst catalytic reaction with an aqueous process is environmentally friendly. Recently, various constructions of mesoporous silica-based heterogeneous catalysts through the immobilization of chiral organometallic complexes onto mesoporous silica materials have obtained great achievements in asymmetric catalysis,[1] in which the most successful examples are based on the understanding of support's function and the controlling of chiral complexation behavior. Mesoporous silica nanospheres (MSNs) are typical supports[2] that have been widely explored. Like the MSNs developed by Zhang and co-workers,[2a] these MSNs possess the general features of typical mesoporous silica materials, such as large specific surface area/pore volume, tunable pore dimension/well-defined pore arrangement and high mechanical stability, making them attractive materials for use as support-matrixes. Furthermore, scalable preparation and easy functionality of these MSNs open up extensive opportunities to immobilize various chiral organometallic complexes. In addition, the unique cooperative assembly possibly constructs uniformly catalytic active species within its silicate network, which is beneficial to mimic a homogeneous catalytic environment. More importantly, cetyl-trimethylammonium tosylate (CTATos), as a structure-directing template agent, often remains within the material during the self-assembly process. This residual CTATos possesses an additional phase transfer functionality that can potentially facilitate a biphasic asymmetric reaction, which is rarely involved in a heterogeneous asymmetric catalysis. Thus, taking advantage of the significant benefits of silica nanospheres, together with these potential functions, it is reasonable to expect that chiral organometal-functionalized mesoporous silica nanospheres have a desired catalytic efficiency both in catalytic and enantioselective performances in a heterogeneous asymmetric catalysis.

Chiral β-trifluoromethylated allylic alcohols, as one of the chiral trifluoromethyl motif family,[3] can be converted into many types of biologically active molecules because of their unique physical and chemical properties in fluorine chemistry.[4] Although many chiral allylic alcohols, obtained by the 1,2-reduction of α,β-unsaturated ketones, are well-documented in the literatures,[5] the construction of chiral β-trifluoromethylated allylic alcohols through the asymmetric reduction of β-trifluoromethylated-α,β-unsaturated carbonyl compounds involvement in the 1,2-reduction of β-trifluoromethylated-α,β-unsaturated ketones is rare in asymmetric catalysis.[6] More importantly, due to these catalytic reactions involving various transition-metal catalysts, the realization of recycle of expensive transition-metal catalysts and the overcoming of product contamination caused by metal leaching are still an unmet challenge. Thus, the exploration of a now immobilization approach to solve these problems is considerably important both in fundamental research, as well as its practical applications.

As part of our ongoing research programs directed to the development of efficiently recoverable heterogeneous catalysts for asymmetric catalysis,[7] herein we report the development of new chiral organoruthenium-functionalized MSNs using the co-assembly of chiral 4-(trimethoxysilyl)ethyl)phenylsulfonyl-1,2-diphenylethylene-diamine and tetraethoxysilane followed by complexation with an organoruthenium complex. As demonstrated in our studies, by taking advantage of the uniformly distributed chiral site-isolated active organoruthenium catalytic nature, it is found that the organoruthenium-functionalized MSNs

Key Laboratory of Resource Chemistry of Ministry of Education, Shanghai Normal University, Shanghai, 200234, China. E-mail: ghliu@shnu.edu.cn Fax: 86-21-64321819;Tel: 86-21-64321819

display high catalytic activity and enantioselectivity in the enantioselective 1.2-reductions of β-trifluoromethylated-α,β-unsaturated ketones to give chiral allylic alcohols in an aqueous medium. Furthermore, this heterogeneous catalyst can be conveniently recovered and reused repeatedly for at least eight times without loss of catalytic activity, rendering it an attractive method in the practice of organic synthesis in an environmentally friendly manner. The outcomes from the study show that this strategy offers a general way to construct other organometal-functionalized MSNs with high catalytic performance.

2. Experimental

2.1. Characterization

Ru loading amounts in the catalysts were analyzed using an inductively coupled plasma optical emission spectrometer (ICP, Varian VISTA-MPX). Fourier transform infrared (FT-IR) spectra were collected on a Nicolet Magna 550 spectrometer using KBr method. Scanning electron microscopy (SEM) images were obtained using a JEOL JSM-6380LV microscope operating at 20 kV. Transmission electron microscopy (TEM) images were performed on a JEOL JEM2010 electron microscope at an acceleration voltage of 220 kV. X-ray photoelectron spectroscopy (XPS) measurements were performed on a Perkin-Elmer PHI 5000C ESCA system. A 200 μm diameter spot size was scanned using a monochromatized Aluminum *Kα* X-ray source (1486.6.6 eV) at 40 W and 15 kV with 58.7 eV pass energies. All the binding energies were calibrated by using the contaminant carbon (C_{1s} = 284.6 eV) as a reference. Nitrogen adsorption isotherms were measured at 77 K with a Quantachrome Nova 4000 analyzer. The samples were measured after being outgassed at 423 K overnight. Pore size distributions were calculated by using the BJH model. The specific surface areas (*S*BET) of samples were determined from the linear parts of BET plots (p/p_0 = 0.05-1.00). Thermal gravimetric analysis (TGA) was performed with a Perkin-Elmer Pyris Diamond TG analyzer under air atmosphere with a heating ramp of 5 K/min. Solid state NMR experiments were explored on a Bruker AVANCE spectrometer at a magnetic field strength of 9.4 T with ^{1}H frequency of 400.1 MHz, ^{13}C frequency of 100.5 MHz and ^{29}Si frequency of 79.4 MHz with 4 mm rotor at two spinning frequency of 5.5 kHz and 8.0 kHz, TPPM decoupling is applied in the during acquisition period. ^{1}H cross polarization in all solid state NMR experiments was employed using a contact time of 2 ms and the pulse lengths of 4μs. Elemental analysis was performed with a Carlo Erba 1106 Elemental Analyzer.

2.2. Catalyst preparation

2.2.1. Preparation of ArDPEN-MSNs (3). In a typical synthesis, 1.92 g (4.22 mmol) of cetyl-trimethylammonium tosylate (CTATos) and 0.35 g (3.27 mmol) of triethanolamine ($TEAH_3$) was dissolved in 100.0 mL of deionized water. The mixture was stirred at 80 °C for 1.0 h. After cooling to ambient temperature, the mixed dual-silane, 12.69 g (61.0 mmol) of tetraethyl-orthosilicate (TEOS) and 4.50 g (9.0 mmol) (*R,R*)-ArDPEN-derived silica (**1**), were added to the solution. The reaction mixture was stirred at 80 °C with a stirring speed of 1200 rpm for another 2 hours. The solids were collected by centrifugation and washed repeatedly with excess distilled water. The surfactant template was removed by refluxing in acidic ethanol (400 mL per gram) for 12 h. The solid was filtered, rinsed with ethanol again, and then dried at 60 °C under reduced pressure overnight to afford ArDPEN-MSNs (**3**) (6.13 g) in the form of a white powder. IR (KBr) cm^{-1}: 3441.5 (s), 2930.1 (w), 2850.1 (w), 1635.0 (m), 1499.2 (w), 1459.5 (w), 1092.1 (s), 956.3 (m), 804.4 (m), 700.3 (m), 564.5 (m). ^{13}C CP/MAS NMR (161.9 MHz): 148.2, 138.3, 127.5 (*C* of of Ph and Ar, and *C* of Ar in CTATos molecule), 70.0-64.9 (*C* of −N*C*HPh−), 59.3 (*C* of –N*C*H$_2$ and –N*C*H$_3$ in CTATos molecule), 34.0-27.5 (*C* of −*C*H$_2$Ar and *C* of –*C*H$_2$– in CTATos molecule), 14.4 (*C* of *C*H$_3$CH$_2$− in CTATos molecule), 8.3 (*C* of −*C*H$_2$Si) ppm. ^{29}Si MAS/NMR (79.4 MHz): T^1 (δ = −53.4 ppm), T^2 (δ = −57.9 ppm), T^3 (δ = −68.6 ppm), Q^2 (δ = −91.3 ppm), Q^3 (δ = −101.6 ppm), Q^4 (δ = −112.1 ppm). Elemental analysis (%): C 26.86, H 4.98, N 4.49, S 3.15.

2.2.2. Preparation of Ru-MSN$_S$ (5). In a typical synthesis, $[RuCl_2(p\text{-cymene})]_2$ (0.32 g, 0.60 mmol) and NEt_3 (0.50 mL, 8.25 mmol) were added to a suspension of **3** (1.00 g) in 20.0 mL of dry CH_2Cl_2 at 20 °C, and the resulting mixture was stirred at 20 °C for 24 h. The mixture was filtered through filter paper and then rinsed with excess CH_2Cl_2. After Soxhlet extraction for 24 h in CH_2Cl_2 to remove homogeneous and unreacted starting materials, the solid was dried at ambient temperature under vacuum overnight to afford catalyst **5** (1.12 g) as a light−yellow powder. ICP analysis showed that the Ru loading-amount was 37.08 mg (0.367 mmol) per gram catalyst. IR (KBr) cm^{-1}: 3441.7 (s), 3057.8 (w), 2961.7 (w), 2922.1 (w), 1635.0 (m), 1507.4 (w), 1499.3 (w), 1459.7 (w), 1387.7 (w), 1092.1 (s), 956.3 (m), 804.4 (m), 700.3 (m), 564.5 (m). ^{13}C CP/MAS NMR (161.9 MHz): 148.1, 137.3, 128.1 (*C* of Ph and Ar, and *C* of Ar in CTATos molecule), 104.2−75.8 (99.8, 87.4, 81.3) (*C*$_6$ of $CH_3C_6H_3CH(CH_3)_2$ in *p*-cymene group), 70.0-64.9 (*C* of −N*C*HPh−), 59.7 (*C* of –N*C*H$_2$ and –N*C*H$_3$ in CTATos molecule), 34.0-27.5 (*C* of −*C*H$_2$Ar and *C* of –*C*H$_2$– in CTATos molecule), 24.7 (*C* of *C*H$_3$C$_6$H$_3$C*H*(CH$_3$)$_2$ in *p*-cymene group), 14.0-23.1 (*C* of CH$_3$C$_6$H$_3$CH(*C*H$_3$)$_2$ in *p*-cymene group and *C* of *C*H$_3$CH$_2$− in CTATos molecule), 8.3 (*C* of −*C*H$_2$Si) ppm. ^{29}Si MAS/NMR (79.4 MHz): T^1 (δ = −53.7 ppm), T^2 (δ = −59.1 ppm), T^3 (δ = −68.9 ppm), Q^2 (δ = −91.3 ppm), Q^3 (δ = −102.3 ppm), Q^4 (δ = −110.2 ppm). Elemental analysis (%): C 37.53, H 5.46, N 3.87, S 2.72.

2.3. General procedure for the asymmetric 1,2-reduction of β-trifluoromethylated-α,β-unsaturated ketones.

A typical procedure was as follows: The catalyst **5** (27.25 mg, 10.0 μmol of Ru, based on ICP analysis), β-trifluoromethylated-α,β-unsaturated ketones (1.0 mmol) and 1.0 mL of HCOOH-NEt_3 (5:2) were added sequentially to a 10.0 mL round−bottom flask. The mixture was then stirred at room temperature (20 °C) for 15−30 h. During this period, the reaction was monitored constantly by TLC. After completion of the reaction, the catalyst was separated by centrifugation (10,000 rpm) for the recycling experiment. The aqueous solution was extracted with ethyl ether (3 × 3.0 mL). The combined ethyl ether extracts were washed with $NaHCO_3$ and brine, and then dehydrated with Na_2SO_4. After evaporation of ethyl ether, the residue was purified by silica gel flash column chromatography to afford the desired product. The

yields were determined by ^{1}H-NMR, and the ee values were determined by a HPLC analysis using a UV-Vis detector and a Daicel OD-H or AD-H chiralcel column (Φ 0.46 × 25 cm).

3. Results and discussion

3.1. Synthesis and structural characterization of the heterogeneous catalyst

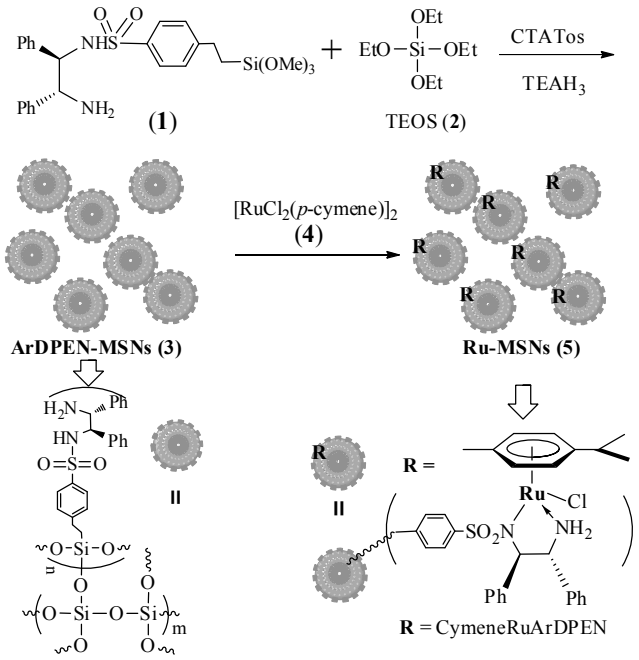

Scheme 1. Immobilization of CymeneRuArDPEN-functionality within the inoganosilicate network.

The incorporation of a chiral CymeneRuArDPEN functionality within its silicate network, abbreviated as Ru-MSNs (**5**), (CymeneRuArDPEN-MSNs:[8] ((η^6-cymene)RuC1[N-((1*R*,2*R*)-2-amino-1,2-diphenylethyl)-4-ethylbenzenesulfonamide], where ArDPEN = N-((*1R,2R*)-2-amino-1,2-diphenylethyl)-4-ethylbenzenesulfonamide) was prepared as outlined in Scheme 1. Firstly, according to the reported method[2a] with the slight modification that the mixed dual silanes (**1** and **2**) were used, the cooperative assembly of **1** and **2** using triethanolamine ($TEAH_3$) and the cationic surfactant counterion cetyl-trimethylammonium tosylate (CTATos) as structure-directing template and surfactant afforded the chiral ArDPEN-MSNs (**3**) as a white powder. Direct complexation of $[RuCl_2(p\text{-cymene})]_2$ (**4**) led to the crude heterogeneous Ru-MSNs (**5**). Finally, this crude material was subjected to Soxhlet extraction to clear its nanochannels and to obtain its pure form as a light-yellow powder (see SI in Figure S1).

Figure 1 showed the FT-IR spectra of the ArDPEN-MSN_S (**3**) and catalyst **5**. Generally, both **3** and **5** exhibited the characteristic bands of the inorganosilicate materials around 3441, 1635 and 1092 cm^{-1} for υ(O−H), δ(O−H) and υ(Si−O), respectively.[9] The relatively weak bands between 3100−2800 cm^{-1} were assigned to the asymmetric and symmetric stretching vibrations of the C−H bonds. The peaks indicative of υ(Si−C) should appear at 1100 cm^{-1}, however, they were difficult to be distinguished because of the overlapping absorbance peaks from υ(Si−O).[10] The bands between 1510−1450 cm^{-1} were attributed to the breathing vibrations of the C=C bonds in the aromatic ring.[9a-b] The intensity of these peaks in catalyst **5** increased consistently relative to those in **3**, implying the coordination of $[RuCl_2(p\text{-cymene})]_2$ occurs. All these observations demonstrated the incorporation of the chiral CymeneRuArDPEN complexes within the MSNs networks.

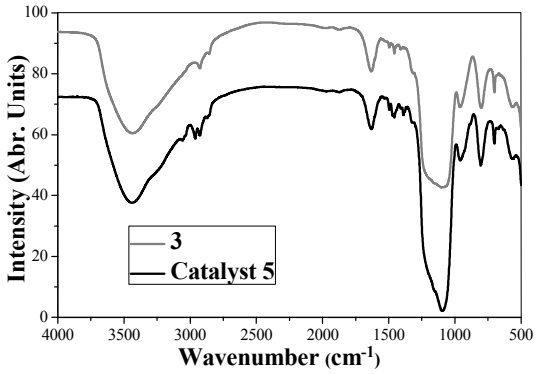

Figure 1. FT-IR spectra of **3** and **5.**

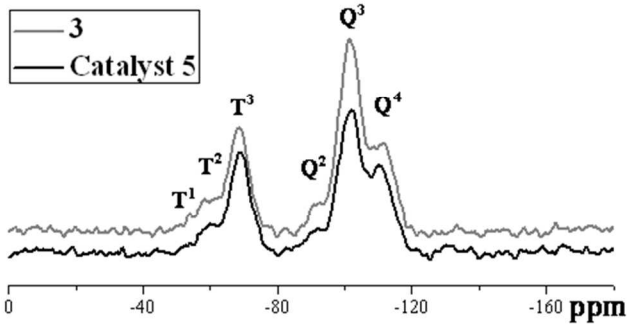

Figure 2. Solid-state ^{29}Si CP/MAS NMR spectra of **3** and **5**.

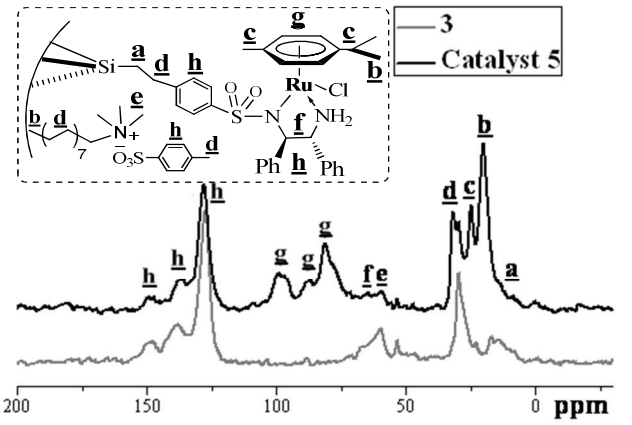

Figure 3. Solid-state ^{13}C CP/MAS NMR spectra of **3** and **5**.

As shown in Figure 2, the ^{29}Si magic angle spinning (MAS) NMR spectra showed that the ArDPEN-MSNs (**3**) and catalyst **5** presented two groups of typical signals (Q- and T-series) that distributed broadly from −50 to −150 ppm, where Q signals were attributed to inorganosilica while T signals were corresponding to organosilica. Typical isomer shift values of catalyst **5** are similar to those reported in the literature[11] (T-series: −48.5, −58.5, and −67.5 ppm for T^1, T^2, and T^3 of [$R(HO)_2SiOSi$], [$R(HO)Si(OSi)_2$], and [$RSi(OSi)_3$], respectively. Q-series: −91.5, −101.5, and −110.0 ppm for Q^2, Q^3, and Q^4 of [$(HO)_2Si(OSi)_2$], [$(HO)Si(OSi)_3$], and [$Si(OSi)_4$], respectively). Notably, strong T signal at −68.9 ppm in the spectrum of **5** was attributed to T^3(R–$Si(OSi)_3$) (R = CymeneRuArDPEN-functionalized alkyl-linked groups), while strong Q signals at at −102.3 and −110.2 ppm in the spectrum of **5** ascribed Q^3 [$(HO)Si(OSi)_3$], and Q^4[$Si(OSi)_4$], respectively. These observations demonstrated that both **3** and **5** possessed the inorganosilicate networks of [$(OH)Si(OSi)_3$] and [$Si(OSi)_4$] with the organosilicate R–$Si(OSi)_3$ species as their main part of silica walls.[12]

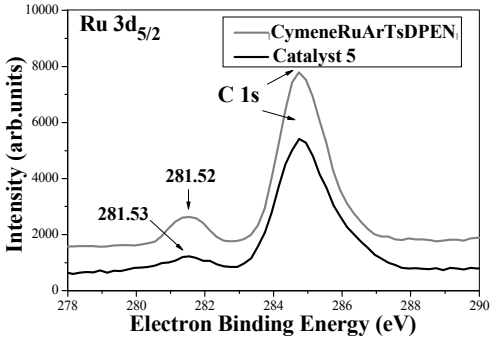

Figure 4. XPS spectra of the homogeneous CymeneRuArDPEN and **5**.

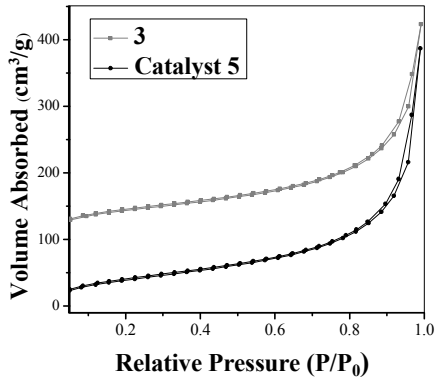

Figure 5. Nitrogen adsorption-desorption isotherms of **3** and **5**.

Incorporation of well-defined single-site active CymeneRuArDPEN center within its silicate network of **5** could be proven by solid-state ^{13}C cross-polarization (CP)/magic angle spinning (MAS) NMR spectroscopy. As shown in Figure 3, both **3** and **5** produced the characteristic carbon signals at ~68 ppm and ~128 ppm, which were corresponded to carbon atoms of the –N<u>C</u>HPh groups and of the –<u>C</u>$_6$H$_5$ groups in ArDPEN moiety, respectively. Peaks between 104.2 and 75.8 ppm in the spectrum of **5** ascribed to the carbon atoms of the aromatic ring in *p*-cymene moiety, while peaks at ~24.7 and ~20.0 ppm in the spectrum of **5** are attributed to the carbon atom of the <u>C</u>H$_3$ and <u>C</u>H groups attached to the aromatic ring in *p*-cymene moiety. These peaks are absent in the spectrum of **3**, suggesting the formation of the CymeneRuArDPEN complex as a single-site center. Chemical shifts of catalyst **5** are strongly similar to those of its homogeneous counterpart CymeneRuTsDPEN,[8a] demonstrating that they had the same well-defined single-site active species. This judgement could be further confirmed by a XPS investigation. As shown in Figure 4, catalyst **5** showed the same Ru $3d_{5/2}$ electron binding energy as its homogeneous counterpart (281.52 eV versus 281.53 eV), in which both were obviously different from that of their parent **4** (see SI in Figure S2), disclosing the well-defined single-site CymeneRuArDPEN active center in catalyst **5** was anchored within its silicate network. In addition, carbon signals of residual CTATos molecule could also be observed (marked in the spectra), which may play an important role in its catalytic performance discussed below.

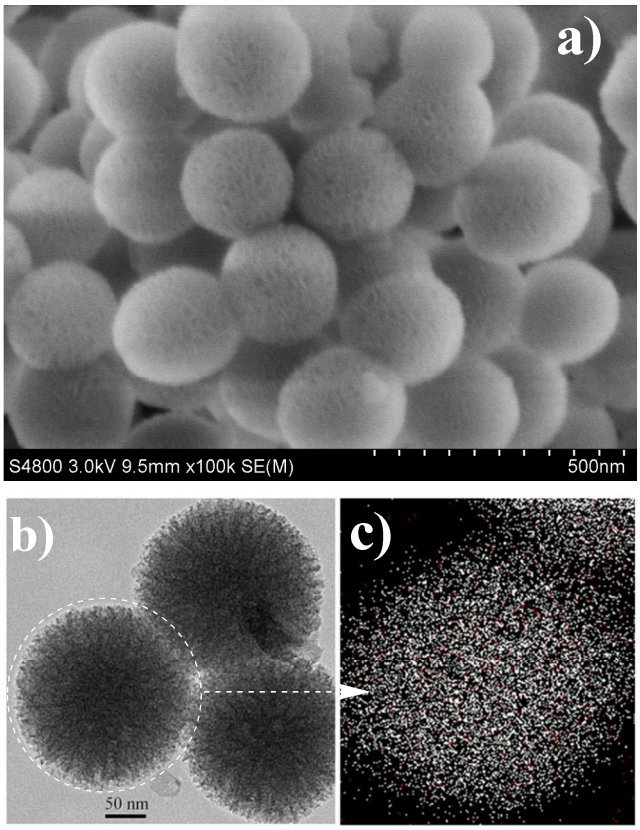

Figure 6. (a) SEM images of **5**, (b) TEM images of **5**, and (c) TEM image with a chemical mapping of **5** showing the distribution of Si (white) and Ru (red)..

The morphology, pore structure and ruthenium distribution were further investigated using nitrogen adsorption-desorption technique, scanning electron microscopy (SEM), transmission electron microscopy (TEM) and TEM with chemical mapping technique. As shown in Figure 5, the nitrogen adsorption-desorption isotherm of catalyst **5** presented a typical IV character with an H1 hysteresis loop, indicating its mesoporous

nanostructure, which was strongly similar to that of the corresponding pure MSN material.[2a] Furthermore, the SEM images revealed that catalyst **5** was composed of the uniformly distributed nanospheres with a particle size of about 250 nm (Figure 6a), which could be further proved by the TEM image (Figure 6b) (for comparison, the SEM and TEM images for **3** could be seen in Figure S3 of SI). In addition, the TEM image with a chemical mapping technique shows that the ruthenium active centers were uniformly distributed within its silicate network (Figure 6c).

These obtained characterizations and analyses demonstrated that the chiral organoruthenium-functionalized mesoporous silica nanospheres possessing an inorganosilicate network of $[(OH)Si(OSi)_3]$ and $[Si(OSi)_4]$, a partially organosilicate wall of consisting of $RSi(OSi)_3$ (R = CymeneRuArDPEN-functionalized alkyl-linked groups), well-defined single-site CymeneRuArDPEN species, and uniformly distributed ruthenium active centers could be readily constructed *via* the co-assembly of the dual-silanes.

3.2. Catalytic performance of the heterogeneous catalyst

3.2.1. Catalytic properties

Chiral N-sulfonylated diamine-based organometallic complexes are well-known to catalyze asymmetric transfer hydrogenation of various ketones,[8, 13] and some have been applied to the enantioselective 1,2-reductions of β-CF_3-substituted-α,β-unsaturated ketones.[6a] In the present study, we have examined the catalytic activity and enantioselectivity of Ru-MSNs (**5**) in the enantioselective 1,2-reduction of 4,4,4-trifluoro-1,3-diphenylbut-2-enone as a model reaction. Reaction with HCO_2H-NEt_3 azeotropic mixture as a hydrogen source and 1.0 mol% of MSNs as a catalyst was investigated according to the reported method.[6a] It was found that the enantioselective reduction of 4,4,4-trifluoro-1,3-diphenylbut-2-enone catalyzed by **5** gave (*R*)-4,4,4-trifluoro-1,3-diphenylbut-2-enol with 98% yield and 97% ee. Such an ee value was comparable to that of its homogeneous counterpart, CymeneRuTsDPEN (Entry 1 vs Entry 1 in brackets, Table 1). In addition, the asymmetric reaction could be run at a much higher substrate-to-catalyst mole ratio without apparently affecting the ee value, as exemplified by the enantioselective 1,2-reduction of benzoylacetonitrile at substrate-to-catalyst mole ratio of 200 (Entry 2, Table 1).

Table 1. Enantioselective 1,2-reductions of β-trifluoromethylated-α,β-unsaturated ketones.[a]

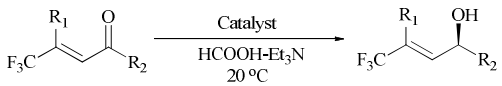

Entry	R_1	R_2	Time(h)	%Yield[b]	%ee [b]
1	Ph	Ph	20 (15)	98(97)	97 (97)[c]
2	Ph	Ph	30	90	96[d]
3	Ph	Ph	20	92	96[e]
4	Ph	Ph	36	95	95[f]
5	*p*-FPh	Ph	20	97	97
6	*p*-ClPh	Ph	20	95	96
7	*p*-BrPh	Ph	20	93	96
8	*p*-MePh	Ph	20	96	96
9	*p*-MeOPh	Ph	20	93	95
10	*p*-CF_3Ph	Ph	24	98	94
11	*o*-MeOPh	Ph	20	99	93
12	Bn	Ph	24	92	89
13	Me	Ph	20	93	92
14	Ph	*p*-ClPh	20	97	93
15	Ph	*p*-BrPh	20	94	94
16	Ph	*p*-MePh	20	93	96
17	Ph	*p*-MeOPh	20	95	97
18	Ph	*m*-FPh	20	95	91
19	Ph	*m*-ClPh	20	94	93
20	Ph	*m*-BrPh	20	93	92
21	Ph	*o*-MeOPh	20	92	94
22	Ph	Me	17	96	29
23	Ph	*t*-Bu	20	93	10
24	*p*-FPh	*p*-BrPh	24	94	92
25	*p*-BrPh	*p*-BrPh	24	92	92

[a] Reaction conditions: catalyst **5** (27.25 mg, 10.0 μmol of Ru based on ICP analysis), β-trifluoromethylated-α,β-unsaturated ketones (1.0 mmol), 1.0 mL of HCOOH-NEt_3 (5:2), and reaction time (15-30 h). [b] Yields were determined by ^{1}H-NMR and ee values were determined chiral HPLC analysis (see SI in Figures S5, S7). [c] Data were obtained in reported literature.[6a] [d] Data were obtained at substrate-to-catalyst mole ratio of 200. [e] Data were obtained using the mixed **3** and its homogeneous CymeneRuTsDPEN. [f] Data were obtained using a parallel CymeneRuArDPEN-SiO_2 as a catalyst.

Based on its high catalytic performance, Ru-MSNs (**5**) was further expanded to the enantioselective 1,2-reduction of a series of β-trifluoromethylated-α,β-unsaturated ketones under the same reaction condition. As shown in Table 1, high yields and high enantioselectivities of the corresponding chiral allylic alcohols could be obtained for most tested substrates. It was noteworthy that the reactions with substrates bearing phenyl groups at R_2 were remarkably enantioselective toward the target products bearing either alkyls or aromatic groups at R_1. Meanwhile, the structures and electronic properties of the substituents on the aromatic rings at R_1 did not significantly affect the enantioselectivities, which were that various electron-withdrawing and -donating substituents on the aryl moiety at R_1

were equally efficient (Entries 5–11). Similarly, in substrates bearing phenyl groups at R_1, the reactions with various aromatic ring at R_2 could be also smoothly transferred to the target products with high enantioselectivities regardless of the presence of electron-withdrawing and -donating substituents on the aryl moiety at R_2 (Entries 14–21). However, when R_2 is an alkyl groups, the reactions afforded the desired chiral products with poor enantioselectivities (Entries 22–23), which may be attributed to the nature of the substrates.[6a] In addition, the reactions with both substrates bearing aromatic rings at R_1 and R_2 were enantioselective toward the target products, in which two representative examples with high enantioselectivities could be observed (Entries 24-25, Table 1).

3.2.2. Investigation of the factors affecting catalytic performance

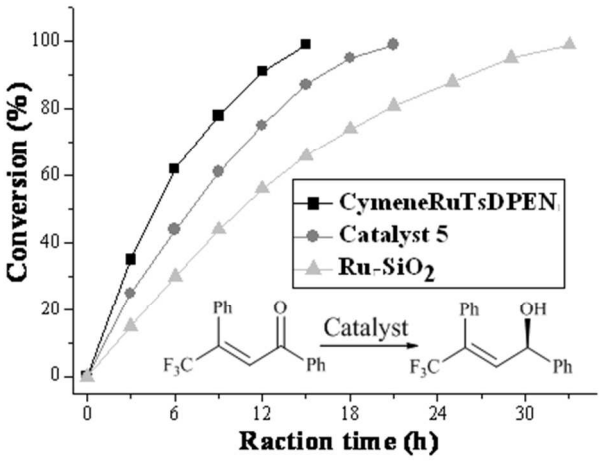

Figure 7. Comparison of the enantioselective 1,2-reduction of 4,4,4-trifluoro-1,3-diphenylbut-2-enone catalyzed by **5**, its inorganosilicate analog (Ru-SiO_2), and the homogeneous catalyst CymeneRuTsDPEN. Reactions were carried out at substrate-to-catalyst mole ratio of 100.

In general, residual homogeneous catalyst *via* a non-covalent physical adsorption in a heterogeneous catalytic system often disturbs a catalytic performance. To eliminate this possibility and to gain insight into the nature of heterogeneous catalysis, one hot-filtration reaction catalyzed by **5** was investigated in the asymmetric enantioselective 1,2-reduction of 4,4,4-trifluoro-1,3-diphenylbut-2-enone. In this case, catalyst **5** was filtered from the reaction mixture after 10 h and the reaction was continued for a further 10 h. It was found that the reaction afforded the corresponding alcohol with 71% conversion and 82% ee in the first 10 h. However, there was no appreciable change both in conversion and ee value in the second 10 h. This finding confirmed that there was no disturbance arising from the homogeneous counterpart *via* a non-covalent physical adsorption, since catalyst **5** had passed through a strict Soxhlet extraction process. This observation disclosed that the nature of this heterogeneous catalysis was indeed derived from the heterogeneous catalyst itself. Further evidence supporting this conclusion came from a parallel experiment. In this case, the asymmetric reduction of 4,4,4-trifluoro-1,3-diphenylbut-2-enone catalyzed by a mixture of **3** and its homogeneous CymeneRuArDPEN was performed. The result showed that the reaction afforded the corresponding alcohol with 92% yield and 96% ee (Entry 3). However, after hot filtration, the reused above mixture gave only tiny products.

Also, it was worth mentioning that the reaction catalyzed by **5** could be completed within 20 h in most cases, which was slightly shorter than that obtained with its homogeneous counterpart (15 h). This characteristic is rare in a generally heterogeneous catalytic system because common heterogeneous catalysts often need significantly longer reaction times than their corresponding homogeneous counterparts. This behavior indicated that the CTATos molecules (cationic surfactant counterion) remaining in its silicate network can serve as phase-transfer function and promote the catalytic performance.[14] In order to confirm the role of the CTATos molecules in catalyst **5,** we prepared an inorganosilicate analog without CTATos molecules within its silicate network. This parallel SiO_2-based CymeneRuArDPEN-functionalized analog, abbreviated as Ru-SiO_2, was obtained through the direct postgrafting of **1** onto SiO_2-based nanospheres using a similar synthetic process (see SI in Figure S4). Using this strategy, we compared its catalytic efficiency with catalyst **5** to understand their different nature in the enantioselective 1,2-reduction of 4,4,4-trifluoro-1,3-diphenylbut-2-enone. The results showed that the reaction catalyzed by Ru-SiO_2 needed 36 h to reach completion in the asymmetric transformation (Entry 4). Notably, the significantly long reaction time relative to that observed with catalyst **5** (20 hours versus 36 hours) demonstrates its lower catalytic efficiency due to the lack of the phase-transfer function of CTATos molecules in the use of Ru-SiO_2 as a catalyst. In other words, the high reaction ratio in catalyst **5** is attributed to the CTATos molecules within catalyst **5**, which significantly promotes the catalytic performance. Further evidence to support this view came from an kinetic investigation in the enantioselective 1,2-reduction of 4,4,4-trifluoro-1,3-diphenylbut-2-enone. As shown in Figure 7, it was found that the asymmetric reduction of 4,4,4-trifluoro-1,3-diphenylbut-2-enone catalyzed by catalyst **5** resulted in an initial activity higher than that achieved with Ru-SiO_2 (the initial TOFs within 1 h were 8.3 and 5.0 $molmol^{-1}h^{-1}$, respectively).

3.2.3. Catalyst's stability and recyclability

Another important consideration in the design of this heterogeneous catalyst is its ease of separation by simple centrifugation, and the used catalyst can retain its catalytic activity and enantioselectivity after multiple recycles. As shown in Table 2, the heterogeneous catalyst **5** was recovered easily and reused repeatedly in eight consecutive reactions using the enantioselective 1,2-reduction of 4,4,4-trifluoro-1,3-diphenylbut-2-enone as a model reaction. After the eighth recycle, catalyst **5** still afforded 91% conversion and 95% ee (see SI in Figure S6). Remarkably, the high recyclability are attributed to the fact that the high dispersive CymeneRuArDPEN active centers *via* strong covalent-bonding immobilization within the MSN network as verified by the SEM chemical mapping can efficiently decrease the leaching of Ru. Evidence to support the view came from the ICP analysis. The amount of Ru after the eighth recycle was 35.15 mg (0.348 mmol) per gram of catalyst and only 5.2% of Ru was lost, demonstrating that its high recyclability was attributed

to the low leaching of Ru.

Table 2. Reusability of catalyst **5** using 4,4,4-trifluoro-1,3-diphenylbut-2-enone as a substrate.[a,b]

Run time	1	2	3	4	5	6	7	8
Conv.[%]	99.9	99.9	99.5	99.7	99.7	98.4	96.3	91.2
ee [%]	97.2	96.9	96.6	96.7	96.5	96.1	95.1	94.9

[a] Reaction conditions: catalyst **5** (272.50 mg, 0.10 mmol of Ru based on ICP analysis), β-trifluoromethylated-α,β-unsaturated ketones (10.0 mmol), 10.0 mL of HCOOH-NEt_3 (5:2), reaction time (20 h). [b] Determined by chiral HPLC analysis.

Conclusions

In conclusions, by taking advantage of a cooperative dual-template approach, we have developed chiral ruthenium-functionalized mesoporous silica nanospheres. As a heterogeneous catalyst, it displays high catalytic activity and enantioselectivity in the enantioselective 1,2-reductions of various β-trifluoromethylated-α,β-unsaturated ketones to give chiral allylic alcohols. As designed, the uniformly distributed, well-defined single-site chiral organoruthenium species could enhance the catalytic activity and enantioselectivity with a range of substrates. Furthermore, this heterogeneous catalyst could be recovered easily and reused repeatedly eight times without any obvious effect on its catalytic performance, which is an attractive feature in the practice of organic transformations. The outcomes from the study suggest we have developed a general approach to the assembly of chiral ligand-derived silane onto functionalized mesoporous silica with significant improvement in catalytic performance in asymmetric synthesis.

Acknowledgements

We are grateful to China National Natural Science Foundation (21402120), Shanghai Sciences and Technologies Development Fund (13ZR1458700 and 12nm0500500), the Shanghai Municipal Education Commission (14YZ074, 13CG48, Young Teacher Training Project) for financial support.

References

1. (a) F. Kleitz, in Handbook of Asymmetric Heterogeneous Catalysis. Wiley-VCH, Weinheim, 2008, pp. 178. (b) D. E. De Vos, M. Dams, B. F. Sels, P. A. Jacobs, *Chem. Rev.*, 2002, **102,** 3615. (c) S. Minakata, M. Komatsu, *Chem. Rev.*, 2009, **109**, 711. (d) M. Bartók, *Chem. Rev.*, 2010, **110,** 1663. (e) A. Mehdi, C. Reye, R. Corriu. *Chem. Soc. Rev.*, 2011, **40,** 563. (f) H. Q. Yang, L. Zhang, L. Zhong, Q. H. Yang, C. Li, *Angew. Chem. Int. Ed.*, 2007, **46**, 6861. g) J. M. Thomas, R. Raja, *Acc. Chem. Res.*, 2008, **41**, 708.
2. (a) K. Zhang, L. L. Xu, J. G. Jiang, N. Calin, K. F. Lam, S. J. Zhang, H. H. Wu, G. D. Wu, B. Albela, L. Bonneviot, P. Wu. *J. Am. Chem. Soc.,* 2013, **135**, 2427. (b) F. Q. Tang, L. L. Li, D. Chen, *Adv. Mater.,* 2012, **24**, 1504. (c) Z. A. Qiao, L. Zhang, M. Y. Guo, Y. L. Liu, Q. S. Huo, *Chem. Mater.,* 2009, **21**, 3823. (d) W. C. Yoo, A. Stein, *Chem. Mater.,* 2011, **23**, 1761. (e) Z. Gao, I. Zharov, *Chem. Mater.,* 2014, **26**, 2030. (f) M. H. Wang, Z. K. Sun, Q. Yue, J. Yang, X. Q. Wang, Y. H. Deng, C. Z. Yu, D. Y. Zhao, *J. Am. Chem. Soc.,* 2014, **136**, 1884. (g) Y. Ma, L. Xing, H. Zheng, S. Che, *Langmuir,* 2011, **27**, 517. (h) D. S. Moon, J. K. Lee, Langmuir, 2012, **28**, 12341. (i) M. J. Stébé, M. Emo, A. F. L. Follotec, L. Metlas-Komunjer, I. Pezron, J. L. Blin, *Langmuir,* 2013, **29**, 1618.
3. (a) R. Filler, Y. Kobayashi, L. M. Yagulpolskii, *Organofluorine Compounds in Medicinal Chemistry and Biomedical Applications,* Elsevier, Amsterdam, 1993. (b) T. Hiyama, *Organofluorine Compounds: Chemistry and Propertie*s, Springer, Berlin, 2000, Chapter 5, pp. 137.
4. (a) J. Nie, H. C. Guo, D. Cahard, J. A. Ma, *Chem. Rev.,* 2011**, 111**, 455. (b) T. Billard, *Chem. Eur. J.,* 2006, **12**, 974.
5. (a) T. Ohkuma, H. Ooka, S. Hashiguchi, T. Ikariya, R. Noyori, *J. Am. Chem. Soc.,* 1995, **117**, 2675. (b) R. Moser, Ž. V. Bošković, C. S. Crowe, B. H. Lipshutz, *Am. Chem. Soc.*, 2010, **132**, 7852. (c) Q. Q. Zhang, J. H. Xie, X. H. Yang, Q. L. Zhou, *Org. Lett.,* 2012, **14**, 6158. (d) N. Arai, K. Azuma, N. Nii, T. Ohkuma, *Angew. Chem., Int. Ed*., 2008, **47**, 7457. (e) T. Konno,T. Takehana, M. Mishima, *J. Org. Chem*., 2006, **71**, 3545. (f) K. R. Voigtritter, N. A. Isley, R. Moser, D. H. Aue, B. H. Lipshutz, *Tetrahedron*, 2012, **68**, 3410. (g) K. A. Nolin, F. D. Toste, *Chem. Eur. J.*, 2010, **16**, 9555.
6. (a) V. Bizet, J. L. Renaud, D. Cahard, *Angew. Chem. Int. Ed.*, 2012, **51**, 6467. (b) Y. Tsuchiya, Y. Hamashima, M. Sodeoka, *Org. Lett.,* 2006, **8**, 4851.
7. (a) H. S. Zhang, R. H. Jin, H. Yao, S. Tang, J. L. Zhuang, G. H. Liu, H. X. Li, *Chem. Commun*., 2012, **48**, 7874. (b) F. Gao, R. H. Jin, D. C. Zhang, Q. X. Liang, Q. Q. Ye, G. H. Liu, *Green Chem.,* 2013, **15**, 2208. (c) R. Liu, T. Y. Cheng, L. Y. Kong, C. Chen, G. H. Liu, H. X. Li, *J. Catal.* 2013, **307**, 55. (d) W. Xiao, R. H. Jin, T. Y. Cheng, D. Q. Xia, H. Yao, F. Gao, B. X. Deng, G. H. Liu, *Chem. Commun.,* 2012, **48,** 11898**.** (e) R. Liu, R. H. Jin, L. Y. Kong, J. Y. Wang, C. Chen, T. Y. Cheng, G. H. Liu, *Chem. Asian. J.* **2013**, *8*, 3108. (f) D. Q. Xia, T. Y. Cheng, W. Xiao, K. K. Liu, Z. L. Wang, G. H. Liu, H. L. Li, W. Wang, *ChemCatChem* **2013**, *5*, 1784. (g). (g) Y. L. Xu, J. Long, K. T. Liu, Q. Q. Qian, F. Gao, G. H. Liu, H. X. Li, *Adv. Synth. Catal*., 2012, **354**, 3250.
8. (a) X. F. Wu, X. G. Li, F. King, J. L. Xiao, *Angew. Chem. Int. Ed.*, 2005, **44**, 3407. (b) T. Ikariya, A. J. Blacker, *Acc. Chem. Res.,* 2007, **40**, 1300. (c) R. Malacea, R. Poli, E. Manoury, *Coordin. Chem. Rev.*, 2010, **254**, 729.
9. (a) A. S. M. Chong, X. S. Zhao, *J. Phys. Chem. B*., 2003, **107,** 12650. (b) Q. Y. Hu, J. E. Hampsey, N. C. J. Li, Y. F. Lu, *Chem. Mater.,* 2005, **17**, 1561. (c) G. Chaplais, J. L. Bideau, D. Leclercq, A. Vioux, *Chem. Mater.,* 2003, **15**, 1950.
10. (a) H. Huang, R. Yang, D. Chinn, C. J. Munson, *Ind. Eng. Chem. Res.,* 2003, **42**, 2427. (b) M. Burleigh, A. Michael, M. Markowitz, S. Spector, B. Gaber, *J. Phys. Chem. B.,* 2001, **105**, 9935.
11. O. Krőcher, O. A. Kőppel, M. Frőba, A. Baiker, *J. Catal.*, 1998, **178**, 284.
12. H. X. Li, Q. F. Zhao, Y. Wan, W. L. Dai, M. H. Qiao, *J. Catal.*, 2006, **244**, 251.
13. (a) J. E. D. Martins, G. J. Clarkson, M. Wills, *Org. Lett.,* 2009, **11**, 847. (b) X. F. Wu, X. H. Li, A. Zanotti-Gerosa, A. Pettman, J. Liu, A. J. Mills, J. L. Xiao, *Chem. Eur. J.,* 2008, **14**, 2209. (c) X. F. Wu, J. Liu, D. D. Tommaso, J. A. Iggo, C. R. Catlow, J. Bacsa, J. L. Xiao, *Chem. Eur. J.,* 2008, **14**, 7699. (d) P. N. Liu, J. G. Deng, Y. Q. Tu, S. H. Wang, *Chem. Commun.,* 2004, 2070. (e) N. A. Cortez, G. Aguirre, M. Parra-Hake, R. Somanathan, *Tetrahedron:Lett.,* 2009, **50**, 2282.
14. V. Cauda, A. Schlossbauer, J. Kecht, A. Zürner, T. Bein, *Am. Chem. Soc.,* 2009, **131**, 11361.